Proceedings of 20th International Congress on Acoustics, ICA 2010

23–27 August 2010, Sydney, Australia

Synthesis of multilayer polymerical nanoparticles using surface acoustic wave atomization

Aisha Qi (1), Peggy Chan (2), Leslie Yeo (1) and James Friend (1)

(1) MicroNanophysics Research Laboratory, Department of Mechanical and Aerospace Engineering, Monash University, Melbourne
(2) Department of Chemical Engineering, Monash University, Melbourne VIC 3800 Australia.

PACS: 43.80.Jz

ABSTRACT

Nanoparticles have been proved to be essentially important for efficient drug deliveries, and the drug particles delivered in-vivo are also required to be biocompatible and biodegradable. Using natural polymers to encapsulate drugs with one or multiple layers offers a likelihood of success in delivering nano-sized drug particles with biocompatible and biodegradable structures. However the techniques at present have yet well-developed and are subject to a number of limitations. In this paper, we present a novel technique about fast synthesizing multilayer polymeric nanoparticles via surface acoustic wave (SAW) atomization. With SAW atomization, we are able to show (1) the successful synthesis of multilayer polymeric structure, and (2) fast generation of monodispersed particles in nanosize. In general, compared to conventional methods in producing nanoparticles, SAW atomization is not only fast and straight forward, but having much less limitations in the usage of surfactant and templates. Compared to traditional ultrasonic atomization and electrospray, SAW atomization, driven at much higher frequency and lower power can not damage biomolecules as easily as the former two.

INTRODUCTION

Current drug delivery technologies and systems remains challenging as having difficulty in (a) delivering drugs with low water-solubility and (b) performing site-targeting deliveries [1]. Applying nanoparticles based technology in this field has offered a likelihood of success in overcoming these challenges. First of all, the dissolution rate of drug particles can be greatly enhanced by using particles with size range in submicron or nanon, and, secondly, nanoparticles can also be modified or coated to target infected organs or tissues [1, 2, 3, 4, 5].

Besides the aspects above, drugs and vaccines delivered in-vivo also requires to be biocompatible and biodegradable. Drug with biocompatibility delivered in-vivo is non-cytotoxic such that the introduction of such material does not invoke a inflammatory response by the immune system. Meanwhile, biodegradable drug can naturally decompose and absorb *in vivo* over a desired period of time such that complicated surgical procedures involved in retrieving or removing such materials are not necessary. Therefore, the encapsulation of bacteria, viruses, DNA, peptides, proteins and other therapeutic molecules within a biodegradable spherical shell of polymeric excipient is a vital vehicle for the controlled and targeted ophthalmic, oral, intravenous or implanted delivery of vaccines and drugs.

Multilayer polymeric encapsulation provides a solution for a more controllable in-vivo drug release, as with such structures, it is able to control over the capsule wall thickness, permeability, stability, and degradation characteristics [6]. A selective polymer for each preferred layer can be designed to be biocompatible and biodegradable for specific parts of body while allowing successive releasing of drugs.

The conventional techniques used for nanoparticle formation and encapsulation all have difficulties in getting nanoparticles with narrow size distribution, unless using emulsion, surfactant and templates. In particular, emulsion based methods, carried out after emulsification/droplet formation process, usually consist of several major complicated steps, all of which require very careful and controlled settings to form homogeneous dispersed single layer particles [7], let alone synthesizing layer-by-layer capsules. The disadvantage of Coacervation/precipitation technique is that it requires to carefully choose right solvents, which can be difficult for adapting itself into various materials, especially for the case of synthesizing LbL particles. Spray drying, usually means ultrasonic atomization and electrospray. These methods seems have less limitation in choosing solvents and the usage of templates is not necessary; however, they, on the other hand, have higher possibility of potentially damaging drugs and other molecules. Ultrasonic atomization, driven at $\sim$10 kHz order, imposes unavoidable shear forces that can damage many shear-sensitive molecules, for example, DNA. Electrospray, on the other hand, driven at $\sim$kV order voltage, still poses high risks of damaging molecules.

Using PDMS microfluidic devices to synthesize polymeric multilayer micro/nanoparticles has become popular recently. The generation of complex emulsions, such as double and triple emulsions, is also achievable with such devices [7, 8]. However, in addition to the drawbacks like other emulsion based methods, other limitations with these devices are: (1) the microchannel surface property is crucial to maintain the desired flow within the microdevice; (2) droplets which form within the microchannels require a cross-linking agent to be solidified into particles; (3) the size of the droplets is limited to the size of microchannels, usually around 50-100 μm, which is too large to be used for drug delivery; and (4) the amount of droplets or particles produced is limited as the droplets/particles are formed one by one.

Therefore, in this study, we present a novel technology to synthesis LbL polymeric nanoparticles via surface acoustic wave (SAW) atomization. It can be categorized as one of the spray drying methods, however, unlike other conventional ultrasonic

atomization, SAW atomization works at much higher frequencies (∼10MHz), meaning the time period of the molecule exposing to the shear force is much shorter than the molecular relaxation time scale in liquids [9, 10] such that the shear effect is greatly minimized [11]. In addition, SAW atomization, compared to electrospray, is driven at very low power (1∼3 W), hardly causing damages to drugs and molecules in a sense of high power and high electric voltage [12, 13].

Surface acoustic wave atomization

Surface acoustic waves (SAWs), with nanometer-order amplitude, can propagate over thousands of wavelengths, typically several centimeters, along the surface in a low loss piezoelectric material like 127.68° y-x cut lithium niobate ($LiNbO_3$ or LN). As its name indicated, the wave amplitude is rapidly attenuated with increasing depth into the LN substrate from the propagation surface. The x-propagating wave speed on the LN substrate c_s is 3965 m/s. When a SAW meets a liquid placed upon the substrate, it diffracts into it at the *Rayleigh* angle, defined by $\theta_R = sin^{-1}(c_w/c_s) \sim 22°$, where c_w, the sound speed in water, is 1485 m/s. The acoustic energy in the liquid causes the bulk recirculation, known as acoustic streaming, within the drop and a body force that causes the drop to translate in the direction of the SAW propagation. At high powers, though the displacement of the surface is only around 10 nm, when the driving frequency is in an order of 10 MHz, the accelerations of the surface is expected to be as high as in an order of 10^7 m/s^2, which, when transmitted into a liquid drop, can induce very strong capillary waves on the drop free surface that are destabilized upon sufficient acoustic excitation. In this manner, a forcing mechanism for rapid and efficient atomization is formed [14], as shown in Fig. 1.

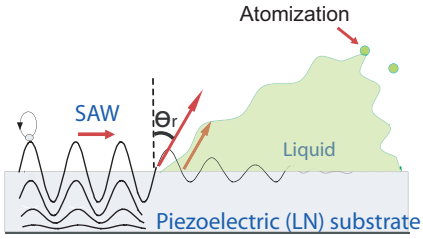

Figure 1: A schematic atomization process [[14, 12]]. SAWs, propagating into a drop at a Rayleigh angle, induce subsequent streaming within the drop and destabilize capillary wave on the free liquid surface. When the power is sufficient, capillary wave breaks up into aerosols, which is known as atomization.

MATERIALS AND METHODOLOGIES

A single-phase uni-directional transducer (SPUDT) was fabricated using sputtering (Hummer®Tripletarget Magnetron Sputter System, Anatech, USA.) and standard UV photolithography with wet-etch techniques onto a 128° y-cut x-propagating lithium niobate ($LiNbO_3$) piezoelectric substrate surface. To achieve the most efficient atomization with limited power input, an enhanced SAW signal, which is located at the focus of the concentric transducers is also achievable by using curved, focusing electrodes. A focusing SPUDT layout is captured under microscope and presented in Fig 2(a). A high frequency electrical signal is supplied to the electrodes, generating mechanical oscillations on the substrate via the inverse piezoelectric effect, thereby inducing a SAW as the efficient atomization driving source [14, 12, 13].

A capillary tube with a tiny paper strip placed at one end was used to supply polymer solutions to the device substrate, as shown in Fig 2(a). As presented in our previous work [13], paper, under SAW excitation, can be used as a convenient media to automatically transport solutions from a reservoir to the device substrate for direct and efficient atomization without damaging the biomolecules. Since the paper strip employed in such setup is very small and the flow rate is also high within the paper such that the amount of molecules that could be left inside the paper is negligible.

The experiment setup can be also shown in Figure 2(b). A capillary tube filled with paper strip is mounted next to the SAW device, where the paper strip is in contact with substrate. A polymer solution is supplied from the other end of the capillary tube. A funnel was placed above the SAW device to collect the aerosols, which, following the air flow provided by a vacuum pump, subsequently passed through a long spiral tube. The spiral tube was fully embedded in a 300 ml hot water buffer and the temperature within the spiral tube is kept between 40–50 degree. The aerosols are dried by evaporation inside the spiral tube, and shrank to small solid particles. These small particles are then deposited into another solution in a glass beaker. Dried particles, will be able to bond to molecules with opposite charge instantaneously. If another layer is required, this suspension, can be collected and re-atomized into another polymer solution again, using the same experiment setup and atomization procedures described above.

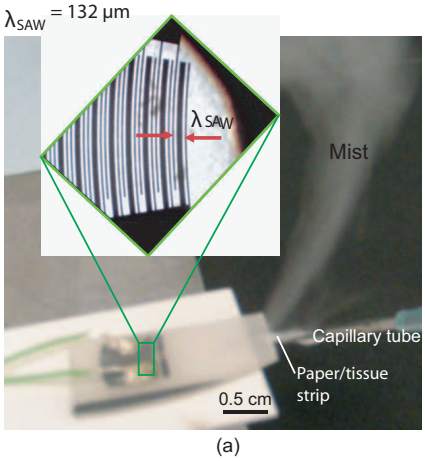

(a)

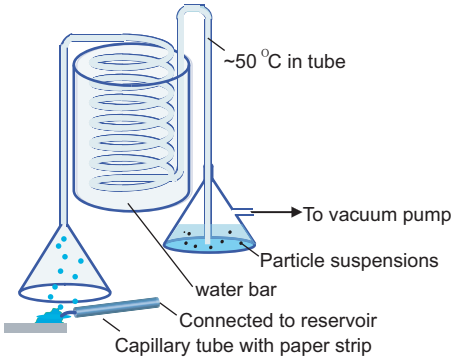

(b)

Figure 2: (a) is a picture of a 30 MHz SPUDT SAW device and its electrode layout captured under microscope. A capillary tube with paper embedded on one end was employed as a liquid supply scheme. (b) A funnel on top is used to collect the mist which can pass through the spiral tube, with the air flow provided by a vacuum pump and then be collected in a beaker.

Model polymers

Chitosan (Chi), a positive charged natural polysaccharide with low cytotoxicity, is one of the most commonly used polymers

which are both biocompatible and biodegradable [15, 16]. It has been proven to be able to efficiently condenses with plasmid DNA and also increase permeability of macromolecules across gastrointestinal tract [17], thus making it an ideal vehicle for gene delivery and vaccines. We therefore select the chitosan (Molecular weight 50k-190k, Sigma) as one of the model polymers.

Carboxymethyl cellulose (CMC), negative charged, is another safe and important artificial-natural polymer derived from cellulose. Polyelectrolyte complex can be formed by the electrostatic interaction between the -COOH group of CMC and the -NH2 groups of chitosan [18, 19]. In this study, we select CMC (Molecular weight 90k, Sigma) as the other model polymer.

Chitosan, was chosen to be the inner polymer layer, while CMC was selected to be the second layer when investigating the size distribution of multilayer polymeric nanoparticle suspension in water using SAW atomization. We also employ chitosan to form a third layer covering CMC when studying the Zeta-potential variation. In this case, CMC was sandwiched between two layers of chitosan. If more layers are required in the real practice, layers can be added one by one using the same technique.

The size of the polymeric particles, d, is defined by $d = c \times D$ [11], where c is the concentration of the polymer and D stands for the size of the aerosol which directly pinched off or ejected from the capillary wave. Based on previous work, D is in an order to 1–10 μm [14, 12]. Aiming at a wide range of drug delivery applications, we expect the size distribution of such particles below micron. We proceeded our experiments with low concentrations of both chitosan and CMC solutions. In particular, we first atomized 0.1 mg/ml$\times$3 ml chitosan solution into 0.01 mg/ml$\times$30 ml CMC solution. This suspension was then re-atomized into another 30 ml chitosan solution with concentration 0.01 mg/ml if another layer is required. In this case, the mass ratio of each polymeric layer was hence theoretically kept at 1:1:1.

Tests on the polymeric particle properties

In order to demonstrate the formation of bonding between polymeric layers, we examined the properties of these LbL capsules such as their fourier transform spectroscopy (FTIR), size distribution and zeta-potential variations.

Proof of the formation of multiple polymer layers

FTIR spectrum was employed to examine the chemical bonding between each polymer layer, thus providing proof of the formation of the different polymer layers. Chitosan-CMC complex spectrum was expected to be varied from the single spectrum of either chitosan or CMC since the bonding between the two would reveal changes. Further evidence of the presence of polymer layering was obtained using zeta-potential measurements (Zetasizer Nano S, Malvern, UK). Pure chitosan is positive charged whilst pure CMC is negative charged. Thus, a change in the sign of the charge, which measured after each layering step, can reveal the formation of a new polymer layer since only the zeta-potential of the outer polymer layer was measurable after complexation between the layers occurs.

Fluorescence labeling

Fluorescence labeling is another method to facilitate visual distinction of the formation of multiple layering. To label the CMC, we employed fluoresceinamine, isomer I N-hydroxy succinimide (NHS) and N-(3-Dimethylaminopropyl)-N-ethylcarbodiimide hydrochloride (EDC). Chitosan, on the other hand, was labeled using NHS-Rhodamine and Dimethylsulfoxide (DMSO). The fluorescence spectra of the different layers during each subsequent layering step can therefore be observed using fluorescence microscopy. In particular, CMC was expected to show green under UV excitation while chitosan should show red under UV excitation. By choosing green and red filters to eliminated interfered lights, green and red particles can be seen respectively.

Particle size distribution

Particle size distribution was obtained using the Zetasizer Nano S (Malvern, UK). The particle size was expected to be around several hundred nanometers after air-drying. Atomic force microscopy (AFM) was also be used to observe individual particle characteristics, from which, the size was also obtained and compared with results from Malvern Zeta-sizer.

RESULTS AND DISCUSSIONS

Bondings between polymeric layers

Fourier transform spectroscopy (FTIR) was employed to examine the chemical bonding between each polymer layer, thus providing proof of the formation of the different polymer layers. Figure 3 shows the FTIR spectrum of polymeric particles. Curves 1 and 2 represent pure CMC and chitosan molecules, respectively, while curves 3 and 4 show the varied spectrum of chitosan-CMC-chitosan triple-layer particle and chitosan-CMC double-layer particle.

From curve 1, the bands at 1154, 1058, and 1026 cm^{-1} are corresponding to the polysaccharide skeletons of CMC. In Chi spectrum (curve 2), the characteristic bands at 1640 and 1558 cm^{-1} are assigned to the amide I and amide II, respectively. The bands at 1052 and 1020 cm^{-1}1 are the characteristic of the polysaccharide skeleton of Chi [20]. Clearly, curves 3 and 4 show characteristic spectrum different from those of Chi and CMC. The amide I band at 1640 cm^{-1} in the double layer and triple layer nanoparticles have shifted to 1660 and 1650 cm^{-1}, respectively, reflecting the interactions between the -COOH groups of CMC and the -NH_2 groups of Chi. The shift in polysaccharide skeleton characteristic bands in the nanoparticles also suggested that ionic complexation between the Chi and CMC has successfully formed.

The variation of Zeta-potential of polymeric particle with different layers serves another proof of bondings. Fig. 4 shows the change of zeta-potential after different polymeric layers was added on one after another by SAW atomization. For both samples 1 and 2, chitosan solution was slightly positive charged. After bonding to CMC with 1:1 mass ratio, an obvious negative charge was obtained, indicating the outer layer of CMC. This sample was re-atomized into chitosan solution and the mass rations of each layer were kept at 1:1:2 for sample 1 and 1:1:1 for sample 2. Clearly, sample 1, with double amount of chitosan at the outer layer, shows a much stronger (nearly double) Zeta-potential compared to sample 1.

In order to visualize different layers of particle, fluorescence microscopy (Olympus BX-51, with UV illuminator U-RFL-T) was employed to observe the particle after fluorescence labeling, as shown in Fig. 5(a)–(c). In particular, Fig. 5(a) shows green light emitted by fluoresceinamine (excitation wavelength 490 nm, emission wavelength 525 nm) labeled CMC component whilst red light in Fig. 5(b) suggests the NHS-Rhodamine (excitation wavelength 540 nm , emission wavelength 625 nm) labeled chitosan. Fig. 5(c) was generated by using software ImageJ (version 1.43r, Wayne Rasband National Institute of Health, USA) to merge Fig. 5(a) and (b). It shows particles are at the same position, suggesting the green and red lights are emitted from the same particle. Therefore, the ionic com-

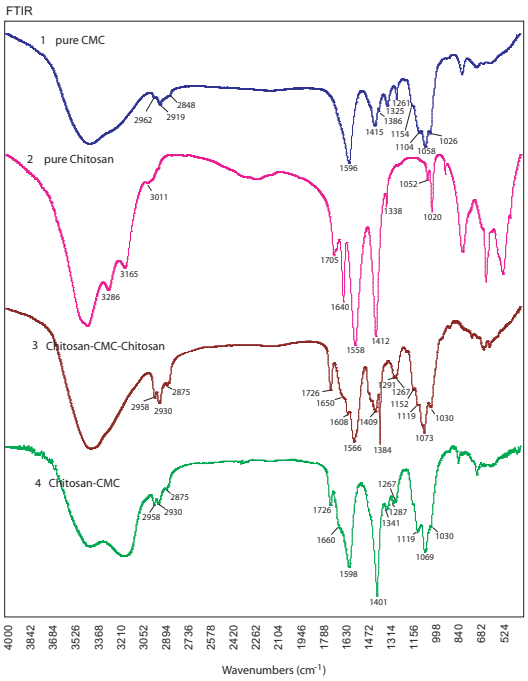

Figure 3: The FTIR spectrum of polymeric particles. Curves A and B are original CMC and chitosan samples, respectively. Curve C represents three-layer particle while curve D shows the spectrum of two-layer particles.

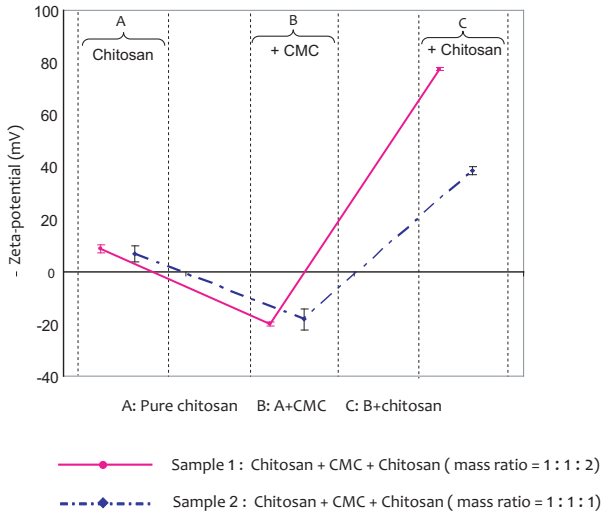

Figure 4: The zeta-potential of multilayer polymeric capsules. For each sample, the zeta-potential varied corresponding to the outlayer of polymer material, suggesting the layers were successfully added one after another as expected.

plexation between chitosan and CMC is successfully formed. In particular, one particle at the top-right corner clearly reveals the red-green light interaction between the CMC and the outer layer chitosan. The possible reason for observing much more red light closed to the outer layer of particle but less close to the inner layer is that the inner layer of chitosan particle was fully encapsulated by the second layer of CMC, thus the light from the former was mostly overwhelmed, or covered, by the latter. In such circumstances, CMC would had less free C-O^{-1} group left to bond with the outer layer chitosan, resulting a weaker layer of chitosan outside. Hence, the green light emitted from the second layer of CMC has greatly interacted with the red light from outer layer of chitosan. Also note that the size of particle showing from these pictures do not stand for the true size distribution as aggregation occurred during days of dialysis after each layering step. More accurate size distribution was obtained right after each layering step, using Zetasizer Nano S (Malvern, UK), shown in the following section.

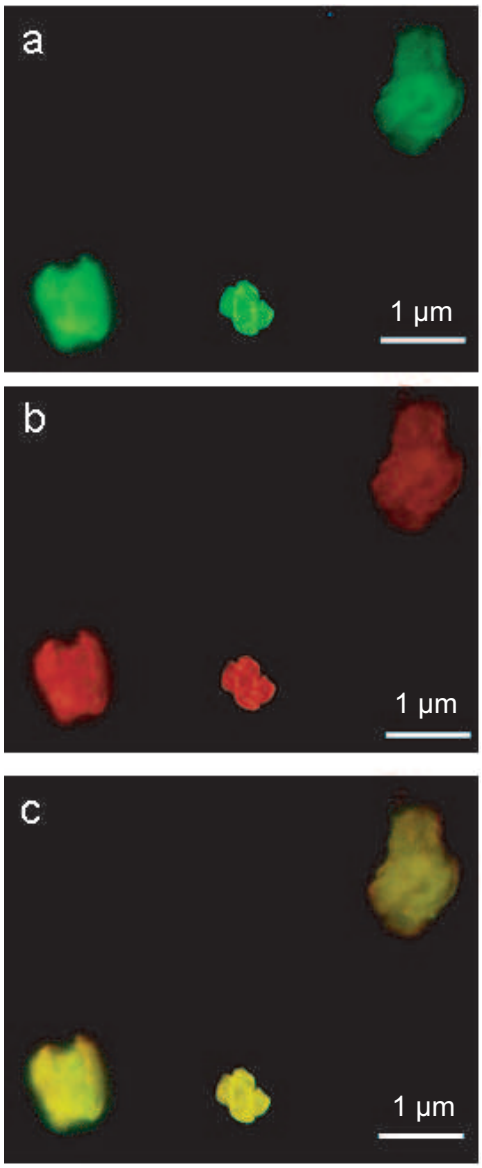

Figure 5: (a) A green filter is used and the green light emitted by fluoresceinamine labeled CMC component is shown. (b) A red filter is used and the red light emitted by NHS-Radamine labeled chitosan is observed. (c) is the combination of the former two, showing the interference between green and red lights, therefore, proving the complexation or bonding between chitosan and CMC.

Size distribution

As discussed in Sec. , nano-sized particles are significantly essential for a wide range of drug delivery administrations. We therefore examined the size distribution of synthesized polymeric particles to see if the size obtained is in the required range, as shown in Figures 6(a) and (b). Samples A and B both represent chitosan/CMC two layer particles (chitosan as the inner core and CMC as the outer layer). Clearly, sample A appeared to be larger (329.9±42.1 nm) than sample B (198.2±7.4 nm). The reason is that when chitosan was first atomized into CMC solution, it was the CMC molecules bonded to dried chitosan particles. The size distribution obtained by Zetasizer is based on Brownian motion such that a layer of molecules on the particle surface will slow the diffusion speed down and the hydrodynamic diameter will therefore be influenced. However, while in sample B, CMC was fully condensed with chitosan particles while drying in the air and the data obtained more accurately represented the true size of dried double layer polymeric suspensions in water (198.2±7.4 nm).

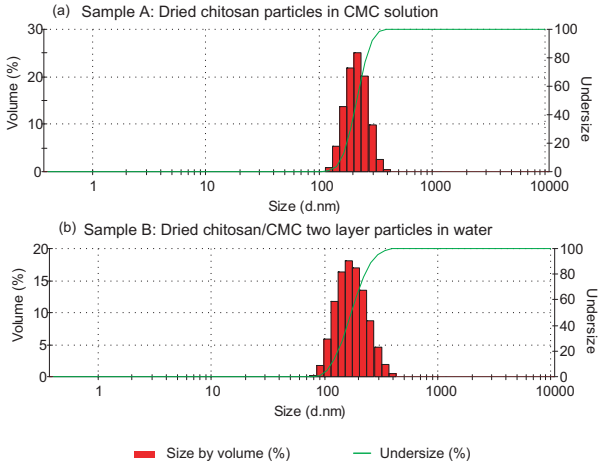

Figure 6: (a) Size distribution of polymeric particle formed after directly collecting dried chitosan particle in CMC solution. (b) Size distribution of the particles from (a) after re-atomization and drying process.

CONCLUSIONS

This paper has demonstrated using SAW atomization as a fast and efficient technique to synthesize multilayer polymeric nanoparticles for drug encapsulation usage. A serial of tests have been conducted and shown the successful bondings between each polymeric layer. The size distribution obtained shows those synthesized multilayer polymeric particles are in a narrow range (around 200 nm), which meets the requirement of many drug administrations (<1 μm). Furthermore, unlike many conventional methods in producing polymeric particles, the usage of surfactant and templates are not required in SAW atomization. Compared to traditional spray drying methods, SAW atomization, driven at much higher frequency and lower power, has much less damage to drugs and vaccines, making it suitable for a wide range of drug deliveries and vaccines.

References

REFERENCES

[1] Kumar, M. N. V. R., ed., 2008. *Handbook of particular drug delivery*. American scientific publishers.

[2] Roney, C., Kulkarni, P., Arora, V., Antich, P., Bonte, F., Wu, A., Mallikarjuana, N., Manohar, S., Liang, H.-F., Kulkarni, A. R., Sung, H.-W., Sairam, M., and Aminabhavi, T. M., 2005. "Targeted nanoparticles for drug delivery through the bloodŰbrain barrier for alzheimer's disease". *Journal of controlled release,* ***108***, pp. 193–214.

[3] Fang, C., Shi, B., Pei, Y.-Y., Hong, M.-H., Wu, J., and Chen, H.-Z., 2006. "In vivo tumor targeting of tumor necrosis factor-?-loaded stealth nanoparticles: Effect of mepeg molecular weight and particle size". *European Journal of Pharmaceutical Sciences,* ***27***, pp. 27–36.

[4] Li, Y.-P., Pei, Y.-Y., Zhang, X.-Y., Gu, Z.-H., Zhou, Z.-H., Yuan, W.-F., Zhou, J.-J., Zhu, J.-H., and Gao, X.-J., 2001. "Pegylated plga nanoparticles as protein carriers: synthesis, preparation and biodistribution in rats". *Journal of controlled release,* ***99***, pp. 203–211.

[5] Koziaraa, J. M., Lockmanb, P. R., Allenb, D. D., and Mumper, R. J., 2004. "Paclitaxel nanoparticles for the potential treatment of brain tumors". *Journal of controlled release,* ***99***, pp. 259–269.

[6] Zelikin, A. N., Li, Q., and Caruso, F., 2008. "Disulfide-stabilized poly(methacrylic acid) capsules: Formation, cross-linking, and degradation behavior". *Chemistry of materials,* ***20***, pp. 2655–2661.

[7] mei Wong, E. H., 2009. "The developement of a continuous encapsulation method in a microfluidic device". PhD thesis, The University of Queensland, Australia.

[8] C.Priest, Quinn, A., Postma, A., Zelikin, A. N., Ralston, J., and Caruso, F., 2008. "Microfluidic polymer multilayer adsorption on liquid crystal droplets for microcapsule synthesis". *Lab on a chip,* ***8***, pp. 2182–2187.

[9] Oxtoby, D., 1981. "Vibrational relaxation in liquids". *Annual Review of Physical Chemistry,* ***32***.

[10] Hsieh, C., Balducci, A., and Doyle, P., 2007. "An experimental study of dna rotational relaxation time in nanoslits". *Macromolecules,* ***40***, pp. 5196–5205.

[11] Alvarez, M., Yeo, L. Y., Friend, J. R., and Jamriska, M., 2009. "Rapid production of protein-loaded biodegradable microparticles using surface acoustic waves". *Biomicrofluidics,* ***3***, p. 014102.

[12] Qi, A., Friend, J. R., and Yeo, L. Y., 2009. "Miniature inhalation therapy platform using surface acoustic wave microfluidic atomization". *Lab on a Chip,* ***9***, pp. 2184 – 2193.

[13] Qi, A., Yeo, L., Friend, J., and Ho, J., 2010. "The extraction of liquid, protein molecules and yeast cells from paper through surface acoustic wave atomization". *Lab on a chip,* ***10***, pp. 470–476.

[14] Qi, A., Yeo, L., and Friend, J., 2008. "Interfacial destabilization and atomization driven by surface acoustic waves". *Physics of Fluids,* ***20***, p. 074103.

[15] He, P., Davis, S. S., and Illum, L., 1998. "Chitosan microspheres prepared by spray drying". *International journal of pharmaceutics,* ***187***, pp. 53–65.

[16] Boonsongrit, Y., Mitrevej, A., and Mueller, B. W., 2006. "Chitosan drug binding by ionic interaction". *European Journal of Pharmaceutics and Biopharmaceutics,* ***62***, pp. 267–274.

[17] Mayank D Bhavsar, M. M. A., 2007. "Polymeric nano- and microparticle technologies for oral gene deliver". *Expert Opinion on Drug Delivery,* ***4***, pp. 197–213.

[18] Anitha, A., Rani, V. D., Krishna, R., Sreeja, V., Selvamurugan, N., Nair, S., Tamura, H., and Jayakumar, R., 2009. "Synthesis, characterization, cytotoxicity and antibacterial studies of chitosan, o-carboxymethyl and n,o-carboxymethyl chitosan nanoparticles". *Carbohydrate Polymers,* ***78***, pp. 672–677.

[19] Zhao, Q., Qian, J., An, Q., Gao, C., Gui, Z., and Jin, H., 2009. "Synthesis and characterization of soluble chitosan/sodium carboxymethyl cellulose polyelectrolyte complexes and the pervaporation dehydration of their homogeneous membranes". *Journal of Membrane Science,* ***333***, pp. 68–78.

[20] Rosca, C., Popa, M. I., Lisa, G., and Chitanu, G. C., 2005. "Interaction of chitosan with natural or synthetic anionic polyelectrolytes. 1. the chitosanŰcarboxymethylcellulose complex". *Carbohydrate Polymers,* ***62***, pp. 35–41.